Aquat. Sci. 65 (2003) 381–398
1015-1621/03/040381-18
DOI 10.1007/s00027-003-0678-1

Aquatic Sciences

Research Article

Characterization of CDOM in an organic rich river and surrounding coastal ocean in the South Atlantic Bight

Piotr Kowalczuk [1, 2, *], William J. Cooper [1], Robert F. Whitehead [1], Michael J. Durako [1] and Wade Sheldon [3]

[1] Center for Marine Science, University of North Carolina at Wilmington, 5600 Marvin Moss Lane Wilmington NC, 28409, USA
[2] Institute of Oceanology, Polish Academy of Sciences, ul Powstańców Warszawy 55, PL-81-712 Sopot, Poland
[3] University of Georgia, Department of Marine Sciences, Athens, Georgia, 30602, USA

Received: 10 May 2003; revised manuscript accepted: 16 August 2003

Abstract. Variability in chromophoric dissolved organic carbon (CDOM) was characterized in and around the Cape Fear River and Onslow Bay, North Carolina USA. The river end member of the study region are extremely rich in CDOM, thus the Cape Fear River serves as a point source of CDOM-rich water into the southeastern Atlantic bight. The river plume is easily traceable and generally extends in a southwesterly direction along the coastline into Long Bay. Depending on physical processes and river flow, the plume can meander somewhat and may even turn northward for short periods of time. The oceanic end member of this study was the Gulf Stream. Samples from the Gulf Stream were obtained up to 97 km off shore. The experimental approach focused on the qualitative and quantitative description of CDOM from fresh-to-oceanic waters. CDOM was characterized by excitation emission matrix (EEM) fluorescence and UV/VIS spectroscopy. Variability of CDOM absorption in the relatively small area of the Cape Fear River estuary and surrounding coastal ocean was very high. The observed range of variability of CDOM absorption coefficient, $a_{CDOM}(350)$, extended over nearly the entire range of CDOM absorption in the literature: $0.046 = a_{CDOM}(350) = 29.9\ m^{-1}$. Changes in CDOM absorption spectrum slope coefficient *S*, were small in the Cape Fear River plume area, but relatively large in Onslow Bay. CDOM EEM spectra indicated that a radical change in composition of CDOM occurs along the river-to-oceanic salinity gradient. CDOM in the coastal ocean was characterized by strong reduction of the three principal intensity peaks: A, C, and M, and a prominent contribution of the T peak to the fluorescence spectrum. The fluorescence intensity is linearly related with absorption. There is a strong inverse relationship between salinity and CDOM absorption, however our data show that this relationship may be dependent on river flow. The distribution of the slope coefficient and the percent contribution of respective peak intensities to the total EEM intensity showed that CDOM undergone conservative mixing until it approached oceanic salinity. Thus, CDOM is so concentrated in the river that mixing and other physical processes mask photochemical or biological alteration of its composition.

Key words. Chromophoric dissolved organic matter; absorption; fluorescence; ocean optics; seasonal variability; estuary mixing processes; South Atlantic Bight.

* Corresponding author phone: +48 58 551 7281 ext. 218;
fax: ++48 58 551 2130; e-mail: piotr@iopan.gda.pl
Published on Web: ■.

Introduction

Dissolved organic matter, DOM, is one of the largest pools of organic carbon in the biosphere and is equivalent in magnitude to terrestrially fixed carbon. In the 300 - 800 nm wavelength range, DOM in surface waters can be divided into transparent and light absorbing groups. The absorbing-fraction, chromophoric dissolved organic matter (CDOM), historically referred to as Gelbstoff, humic matter, or yellow substances, is the primary absorber of sunlight and a major factor that determines the optical properties of natural waters and directly affects both the availability and the spectral quality of light. The optical properties of CDOM may also serve to protect organisms against damaging light effects. At higher concentrations, CDOM absorption extends to visible wavelengths and may inhibit primary production. CDOM is thought to be important for most photochemically-mediated processes in surface waters. Through these processes it may stimulate or deter biological activity or both (for a review see, Mopper and Kieber, 2002). CDOM can also be a source of reactive oxygen species in marine waters (e.g., Cooper et al., 1989; Del Vecchio and Blough, 2002b; Kieber et al., 2003; Whitehead and de Mora, 2000). Thus interest in CDOM and its characterization have increased recently for several reasons: 1) remote sensing of ocean color, related to organic carbon cycling; 2) remote sensing of chlorophyll as an indicator of primary productivity and the potential interference in its measurement by CDOM; 3) air-sea exchange of important trace gases, namely CO, CO_2 and COS; 4) the formation of reactive oxygen species and their potential impact on biological processes and geochemical cycling; 5) as a tracer of riverine input of organic carbon to the ocean; 6) carbon cycling in coastal waters, and; 7) attenuation of ultraviolet light in surface waters.

CDOM absorption decreases exponentially toward longer wavelengths and can be described by the exponential equation (Jerlov, 1976; Kirk, 1994):

$$a_{CDOM}(\lambda) = a_{CDOM}(\lambda_0)\, e^{-S(\lambda_0-\lambda)} \quad (1)$$

where: $a_{CDOM}(\lambda)$ is the absorption coefficient at wavelength λ, λ_0 is a reference wavelength, and S is the slope coefficient (the exponential decrease of the absorption spectrum over a given wavelength range). These parameters describe CDOM quantitatively and can be used to estimate the entire absorption spectrum from equation (1) if absorption at the fixed (reference) wavelength and S are known.

The absorption of light by CDOM affects both the inherent and apparent optical properties of seawater. Therefore, optical methods, including remote sensing, may be applied to study the distribution of CDOM in the ocean. The highest concentrations of CDOM are found in coastal margins of oceans and in semi-enclosed seas where direct sources of terrestrial organic matter are found. These waters are usually classified optically as Case 2 waters (Morel and Prieur, 1977), where interactions of the natural light field with optically-active components of seawater are very complex, making the application of CDOM mapping by remote sensing very difficult. Moreover, the high spatial and temporal variability of CDOM in these regions limits remote-sensing algorithms for CDOM to local areas. Kahru and Mitchell (1999, 2001) have recently presented examples of remote-sensing algorithms for estimation of CDOM in the coastal ocean. They successfully applied SeaWiFS imagery to studies of the spatial and temporal variability of CDOM in the California Current. Similar approaches of using the empirical relationships to link CDOM absorption with apparent optical properties have been used by Kowalczuk et al., (2003) in the Baltic Sea to estimate CDOM absorption as a function of diffuse attenuation coefficient and spectral reflectance. In clear oceanic water, optical Case 1, it is possible to estimate the CDOM signal with semi-analytical modeling (e.g., Garver and Siegel, 1997).

The fluorescent properties of CDOM have been known for a long time (Duursma, 1965) and the fluorescence signal has been used to estimate of CDOM in marine waters (e.g., Højerslev, 1989). The first report of its use in the Cape Fear River plume was by Willey and Atkinson (1982). Numerous investigators have observed the linear relationships between fluorescence and absorption over the past 10 years (Ferrari and Tassan, 1991; Hoge et al., 1993; Vodacek et al., 1997; Ferrari and Dowell, 1998; Ferrari, 2000). A linear relationship was also demonstrated between fluorescence and the formation of reactive oxygen species (Shao et al., 1994). Recent advances in fluorescence spectroscopy have resulted in a new technique called Excitation Emission Matrix (EEM) fluorescence spectroscopy (3-D fluorescence). EEM spectra are obtained by acquiring emission spectra at a series of successively longer excitation wavelengths. The emission spectra are concatenated to generate a plot in which the fluorescence is displayed as the function of excitation and emission wavelengths. Although slower to collect, EEM spectra provide a more complete picture of CDOM emission properties and can often be used to discriminate among different classes of fluorophores based on their excitation/emission maxima. It is also possible to use EEM to follow changes in CDOM resulting from biological or physical processing of the material. Coble (1996) was the first to successfully apply this technique to field data analysis with descriptions of CDOM in the Caribbean, Arabian Sea and Gulf of Mexico (e.g., Coble et al., 1998; Del Castillo et al., 1999; Del Castillo et al., 2000).

CDOM distribution and optical properties are influenced by physical, chemical and biological processes

which contribute to its formation, transformation and degradation. The origin and fate of the CDOM is a matter of discussion. It is widely accepted that most of the CDOM in coastal environments has a terrestrial origin and is transported to the ocean via rivers. The geographical extent of the terrestrially-dominated regions varies seasonally, depending on the magnitude of freshwater inputs (Blough et al., 1993; Nelson and Guarda 1995; Vodacek et al., 1997; Rochelle-Newall and Fisher, 2002b). On local scales, in situ production from phytoplankton decomposition and extraction from bottom sediments may be an important source of CDOM (e.g., Kowalczuk, 1999; Kahru and Mitchell, 2001; Twardowski and Donaghay, 2001; Boss et al., 2001). In the central, oligotrophic regions of the oceans, CDOM is presumably created in situ by as yet poorly understood processes. However, recent observations have shown that CDOM absorption does not correlate with chlorophyll-a content (e.g., Nelson et al., 1998; Rochelle-Newall et al., 1999; Rochelle-Newall and Fisher, 2002b). So, it has been proposed that phytoplankton do not produce CDOM directly, but act as a source of biomass that is transformed to CDOM via microbially-mediated processes (e.g., Tranvik, 1993; Tranvik and Bertilsson, 2001; Rochelle-Newall and Fisher, 2002a). These reports and the earlier work (e.g., Harvey et al., 1983; Kieber et al., 1997), suggest a complicated, and ill-defined pathway of CDOM formation with precise mechanism(s) and rates as yet to be determined in oceanic regions.

It is assumed that CDOM is removed from water in three ways: coagulation and precipitation of the high molecular weight fraction of terrestrial DOM, microbial uptake, and/or photochemical reactions. Coagulation and precipitation within estuaries is an effective pathway for the removal of high molecular weight humic substances (Pempkowiak, 1988); however, recent studies provide evidence that precipitation has a small impact on CDOM optical properties (Blough et al., 1993; Del Castillo et al., 2000). Bacterial uptake is considered an important sink of CDOM; however, studies indicate that it is an indirect process. The organic matter derived from CDOM becomes available for microbial consumption after alteration by photochemical processes (e.g., Moran et al., 2000). Recently, a large number of field and laboratory studies have shown that photobleaching alone is a large sink of CDOM with half-lives ranging from hundreds to thousands, of hours. The prominent effect of CDOM photobleaching is an increase in the slope of the absorption spectrum mainly due to relatively faster photobleaching in the UV-A (Vodacek et al., 1997; Nelson et al., 1998; Grzybowski, 2000; Whitehead et al., 2000; Twardowski and Donaghay, 2001; Twardowski and Donaghay, 2002).
The South Atlantic Bight (SAB), defined herein as the shoreline and the continental shelf from Cape Hatteras to Cape Canaveral, is mostly coastal plain that grades gently into a wide (50-100 km) shelf. The wide shelf is bordered on its east by the Gulf Stream. Much of the shoreline consists of barrier inlands separated by shifting inlets and backed by riverine estuaries, sounds, lagoons, salt marshes and the Intracoastal Waterway. Riverine input is sporadic. Some areas like portions of Onslow Bay are sediment-starved with little riverine input, whereas just to the south is North Carolina's largest and most industrialized riverine system, the Cape Fear River watershed. This river drains directly into the coastal ocean off of North and South Carolina (Mallin et al., 2000). The entire region is subject to frequent flooding, numerous catastrophic storms and chronic erosion problems. Summaries of a number of previous studies of physical, chemical and biological properties of the continental shelf of the South Atlantic Bight are given by Atkinson et al. (1985).

Due to the social and economical importance of the Carolinas' coastal region, environmental monitoring is increasingly important in the SAB. The University of North Carolina at Wilmington has begun an inter-disciplinary, long-term Coastal Ocean Research and Monitoring Program, CORMP, to understand the physical, biological, chemical and geological aspects of this southern region, as well as impacts of natural and anthropogenic changes on the coastal-ocean resources and their management. One of the objectives within CORMP is the optical characterization of the waters of Onslow Bay, the Cape Fear River Plume and coastal southeastern North Carolina. Changes in the optical properties of water masses may be used to compare physicochemical processes within, and exchange between, the coastal system of Onslow Bay and the adjacent estuarine system of the Cape Fear River plume. Coastal and estuarine waters differ greatly in their inherent and apparent optical properties. In the coastal ocean, clear water, low in particle loads and phytoplankton pigment concentrations, comprising the optical characteristics of Case 1 waters, may be found a few km offshore. In areas influenced by riverine inflow, water optical properties are determined by high CDOM and sediment input as well as enhanced phytoplankton growth. These waters may be classified optically as Case 2 waters. The Cape Fear River serves as a point source of water into the southeastern Atlantic bight and the river end members of the study region are extremely rich in CDOM. Therefore, the characterization of CDOM in these waters is extremely important for understanding the coupling between CDOM and conditions for phytoplankton growth and the impact of CDOM on inherent and apparent optical properties of the SAB. In situ optical measurements are needed to compare with estimates derived from SeaWiFS imagery to build a database for refining regional bio-optical models. These data could also be used for further improvement of the accuracy of remote sensing algorithms for chlorophyll and regional

estimates of phytoplankton production. Reports on optical properties in the SAB are scarce (Nelson and Guarda, 1995) so this experimental data set will be a valuable addition.

In this study, we focused on investigating the quantitative and qualitative changes in CDOM on its pathway from fresh to open-ocean waters, as well as the transformation in CDOM composition with the use of EEM.

Materials and methods

This report describes a study period from October 2001 to January 2003. River plume samples were collected from a sample grid developed for the CORMP program, (see Fig. 1). This grid consists of 7 stations (marked as blue dots and labeled CFP1 through CFP7) located at the Cape Fear River mouth. The grid was designed to study the spatial and temporal extent of the Cape Fear River plume. Onslow Bay samples were collected along a transect consisting of 14 stations (marked as red dots and labeled OB) starting at the sea buoy of Masonboro Inlet and extending southeast across the continental shelf to its break at station OB63. The Cape Fear River plume area was sampled monthly (depending on weather) at ebb tide, for maximum extent of the plume. The Onslow Bay transect was sampled monthly in the 2001, and every second month from April 2002. Surface water samples were collected at all stations in the plume grid and on selected stations across Onslow Bay. Initially, water samples were collected at stations OBSB, OB15, OB27, OB42, OB57, OB63. After preliminary data analysis of Onslow Bay data the sampling strategy was changed in April 2002, and samples are now collected at every station from OBSB to OB27 to achieve better resolution of spatial variability. All field operations were performed using small vessels: R/V Sturgeon (9 m) for the Cape Fear River plume and R/V Cape Fear (21 m) for Onslow Bay. Both vessels are too small to install permanent wet laboratories, therefore, water samples for CDOM spectroscopic analysis were collected using a pre-rinsed bucket, and stored in HDPE bottles in ice coolers and processed in the laboratory the following day. HDPE bottles were flushed with a high volume of DI water, and then rinsed several times with the marine sample water from each site, prior to sample storage. Surface salinity was measured with a YSI handheld CT meter or a Seabird CTD and expressed in practical salinity units (PSU).

Samples for spectroscopic analyses were first warmed to room temperature and filtered through ~0.7 µm GF/F filters to remove the large particles and phytoplankton cells then filtered again through 0.2 µm, acid-washed and Milli-Q rinsed Gelman Supor® polysulfone filters. Absorbance scans from 240 to 800 nm, 1 nm slit width, were made using 10 cm Suprasil cuvettes on a Cary 1E dual-beam spectrophotometer connected to a micro-computer. Pre-filtered (0.2 µm) Milli-Q water was used in the reference cell. Absorbance measurements at

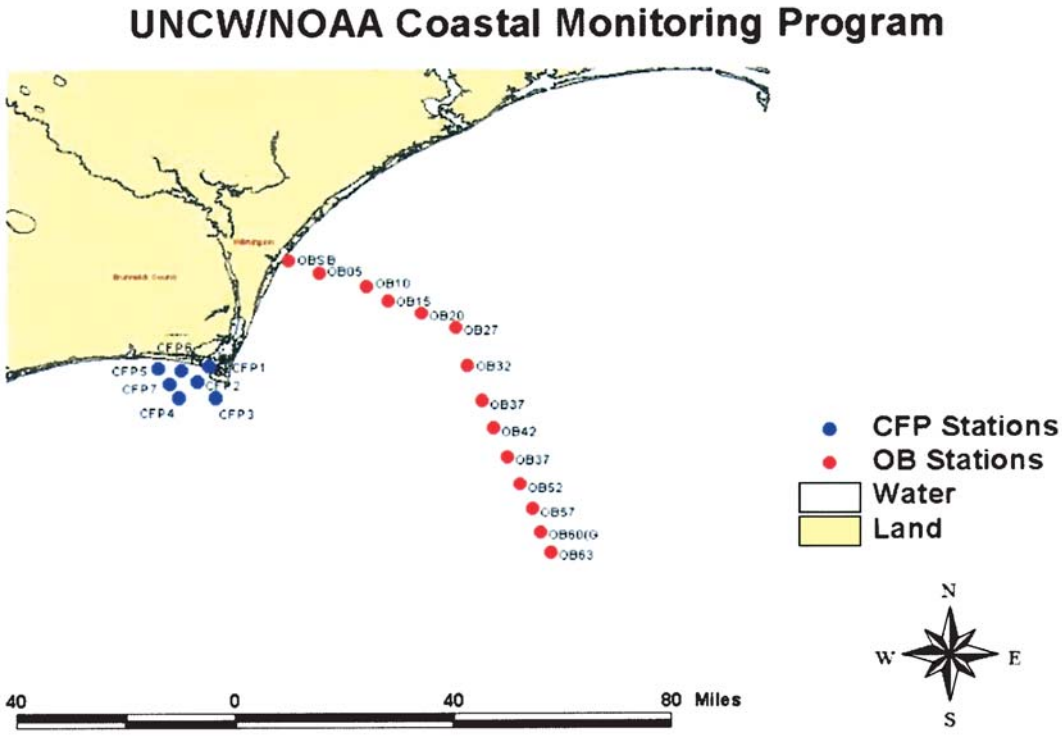

Figure 1. Location of sampling stations in the Cape Fear River plume area and in Onslow Bay.

each wavelength (λ) were baseline corrected by subtracting the mean absorbance calculated in the spectral range from 650 to 700 nm. The required corrections were generally less than 0.002. CDOM absorption coefficients ($a_{CDOM\ \lambda}, m^{-1}$) at each wavelength ($\lambda$) were calculated according to Kirk, (1994):

$$a_{CDOM\,\lambda} = 2.303\ A_\lambda / l \quad (2)$$

where, A_λ is the corrected spectrophotometer absorbance reading at wavelength λ and l is the optical path length in meters. A conservative detection limit of 0.046 m^{-1}, corresponding to 0.002 with 10 cm cells on the spectrophotometer, was estimated from repeated scans of Milli-Q water processed as a sample. The detection limit corresponds to the absorbance at wavelengths in the range of 450 nm for the clearest samples in Onslow Bay to 600 nm for the Cape Fear River plume samples. Following the recommendations of recent studies (see: Stedmon and Markager, 2001; Blough and Del Vecchio, 2002), the spectral slope of the absorption spectrum S was calculated by applying a simple exponential model to fit the offset-corrected absorption spectrum at a spectral range from 300–500 nm. This method of spectral slope calculation is less dependent on the spectral range used. The spectral range was reduced (300–450 nm) for the clearest samples collected at the shelf break, because of the very low absorption at longer wavelengths.

Samples for fluorescence were treated in the same manner as those for absorbance measurements. Highly-absorbing samples were diluted with Milli-Q water to the point where A_{350} (1 cm path length) was ≤ 0.02 to minimize inner-filtering effects. Excitation-emission matrix (EEM) fluorescence properties were determined on a Jobin Yvon SPEX FluoroMax-3 scanning fluorometer equipped with a 150 W Xe arc lamp and a R928P detector. EEM were constructed by using excitation wavelengths from 250 to 500 nm (5 nm intervals) and scanning emission wavelengths from 280 to 600 nm (5 nm intervals). The instrument was configured to collect the signal in ratio mode with dark offset using 5 nm bandpass on both the excitation and emission monochromators. Scans were corrected for instrument configuration using factory-supplied correction factors, which were determined essentially as described in Method 1 of Coble et al., (1993). Post processing of scans was performed using FLToolbox 1.91 developed by Wade Sheldon (University of Georgia) for MATLAB® (Release 11). The software eliminates Rayleigh and Raman scattering peaks by excising portions (± 10–15 nm FW) of each scan centered on the respective scatter peak. The excised data were replaced using three-dimensional interpolation of the remaining data according to the Delaunay triangulation method and constraining the interpolation such that all non-excised data were retained. Following removal of scatter peaks, data were normalized to a daily-determined water Raman intensity (275ex/303em, 5 nm band pass) and converted to Raman-normalized quinine sulfate equivalents (QSE) in ppb (Coble et al., 1998). For samples that required dilution, the scatter-corrected fluorescence of the diluent Milli-Q was subtracted and the resultant fluorescence values were multiplied by the dilution factor to obtain the intensity for the original, undiluted sample. Replicate scans were generally within 5 % agreement in terms of intensity and within-bandpass resolution in terms of peak location. Peak locations are labeled as defined in Coble (1996). The post-processing software did not adequately correct for second-order Raman scattering. The tail of second order Raman scattering was visible at low signal samples. That error was corrected by subtracting the EEM spectrum of the blank sample of freshly prepared Milli-Q water, measured separately for each data series. After correction, EEM and specific peak areas were integrated using procedures available in the FLToolbox package. The same integration procedure and peak areas were used for all samples analyzed in this study.

A crucial issue for the data analysis described above is the selectivity of the scattering correction procedures, because tyrosine- and tryptophan-like peaks (T peak) are located very close to the Raman scattering line. We performed a simple comparison to test the selectivity of the scattering removal and location of the T peak. First, we ran solutions (0.1 mg/L) of tyrosine and tryptophan in Milli-Q water. The EEM spectra were treated as regular samples and all scattering correction routines were applied. The tyrosine and tryptophan peaks were in the exact positions as specified in Coble et al. 1998 (Fig. 2). A second test for the scattering correction procedures was to subtract a fluorescence signal, expressed in counts per seconds, of blank sample (Milli-Q water) from a raw (cps), unprocessed signal of the analyzed sample. Then, peak locations were compared with peaks visible on the EEM spectrum of the same sample processed with the FLToolbox package. No differences were observed (see Fig. 3) allowing us to proceed with further studies using this software.

Results

Quantitative description of CDOM changes in the study area

It is widely accepted that CDOM absorption can be used as a proxy for DOC concentration and that spectral slope can be used as a proxy for the composition of CDOM. We chose the CDOM absorption coefficient at 350 nm, $a_{CDOM}(350)$, for describing changes in CDOM quantity and the CDOM absorption spectrum slope coefficient S, to differentiate CDOM pools. EEM were also used to detect the qualitative changes in CDOM composition. Over

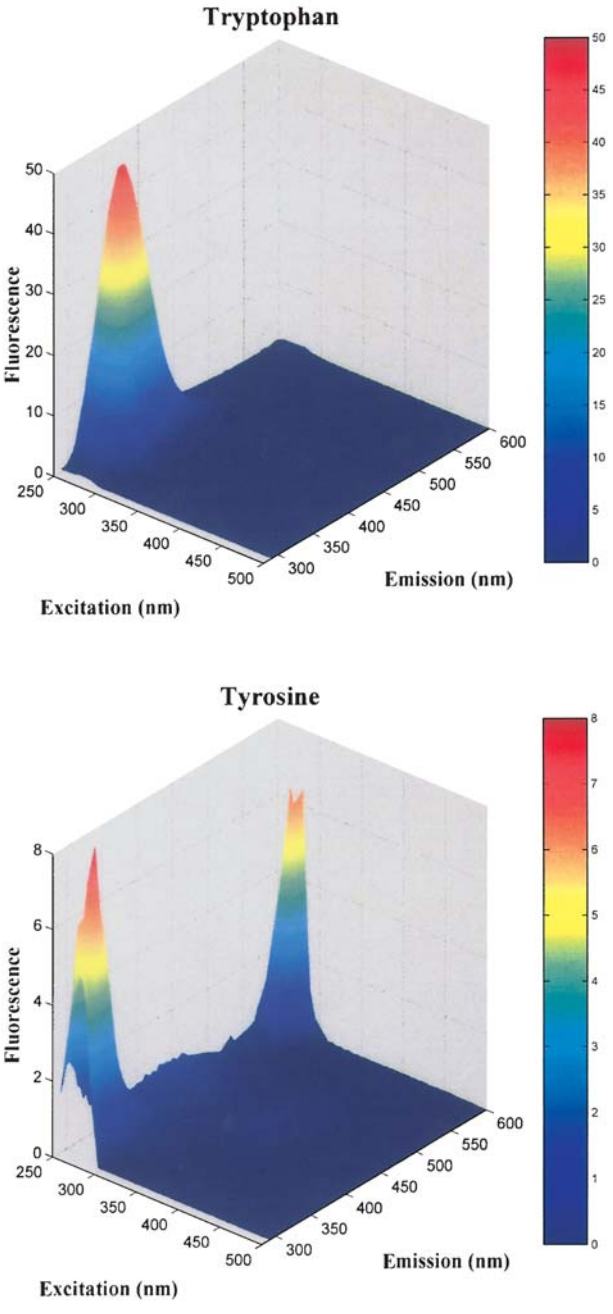

Figure 2. EEM spectra of pure tryptophan and tyrosine dissolved in Milli-Q water at the concentration of 0.1 mg/L.

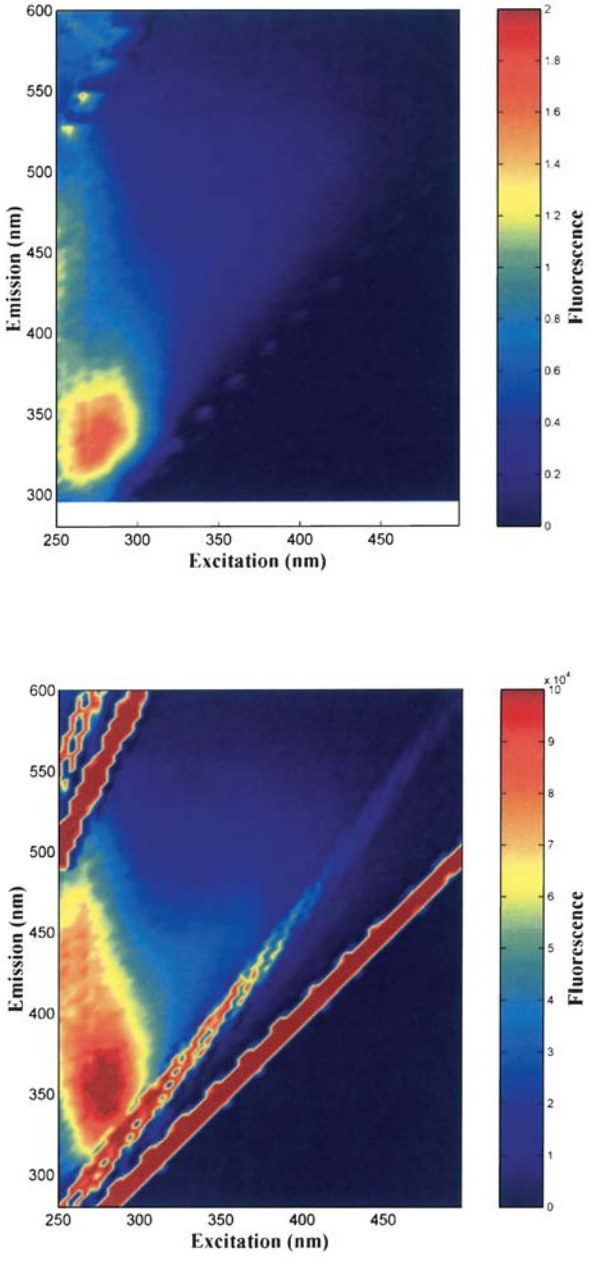

Figure 3. Comparison of EEM spectra of water sample collected on the station OB27, on Sept. 5, 2002. Upper graph shows the fluorescence spectra corrected for Raleigh and Raman scattering (the fluorescence intensity expressed in QSE units) with use of the correction protocols included at FLToolbox software. Lower graph shows the same spectrum as the raw, uncorrected data, (the fluorescence intensity expressed as counts per second – numbers of photons reaching detector in the time unit). Note the distinctive T peak is clearly visible on corrected and raw EEM.

the time period this observation program, we collected 105 samples for CDOM absorption and 105 for EEM analysis, 60 in the Cape Fear River Plume and its estuary and 45 in Onslow Bay. Examples of CDOM absorption spectra for respective sampling areas are shown in Figure 4.

The overall range of CDOM absorption coefficients in the study area was nearly four orders of magnitude. The freshwater end member (salinity = 0) in our data was represented by a sample collected in the October 2001 in the Black River, a tributary of the Cape Fear River. The CDOM absorption coefficient, $a_{CDOM}(350)$, was 29.9 m^{-1}, and the CDOM absorption spectrum slope coefficient S, was 0.015 nm^{-1}. The absorption coefficient of four samples collected in the Cape Fear River estuary between Wilmington and Fort Fisher ranged between $6.01 \leq a_{CDOM}(350) \leq 10.35$ m^{-1}, but the slope coefficient S varied

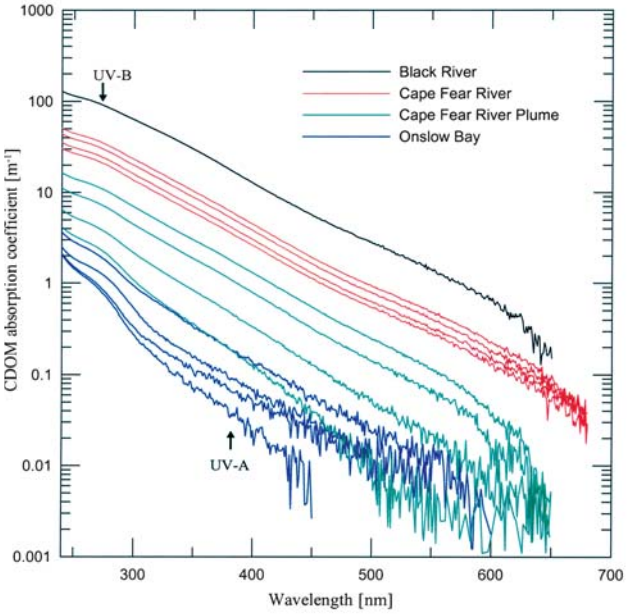

Figure 4. Examples of CDOM absorption spectra in the study area collected during the experiment in Onslow Bay, the Cape Fear River plume, and the Cape Fear River estuary.

little, $0.0154 \le S \le 0.0156$ nm^{-1}, and was similar to S calculated for the Black River.

The distribution of values of CDOM absorption coefficient, $a_{CDOM}(350)$, and CDOM absorption spectrum slope coefficient S, and Cape Fear flow data (daily average for a specific sampling date, in m^{3}s^{-1}) are given in Table 1. Two data sets collected in Onslow Bay have been excluded from cruise-to-cruise comparison. The absorption signal observed in the offshore stations in Onslow Bay in December 2001, was extremely low, $a_{CDOM}(350) \approx 0$ m^{-1}, leading to uncertainty in the slope coefficient calculation, which resulted in unrealistically high values. The cruise in January 2002, was shortened due to adverse weather conditions, and too few samples were collected to calculate the statistical parameters. However, these data and inshore samples from December 2001 have been included in the general statistics.

CDOM absorption in the plume area exhibited high variability, nearly one order of magnitude, caused by fluctuations in river flow (Table 1). During high-flow conditions, the spatial extent of the plume covered the entire sampling grid; CDOM absorption levels were elevated and comparable with those from the estuary. During low-flow conditions, the plume was restricted to the river mouth and CDOM absorption was lower. The $a_{CDOM}(350)$ values at the offshore stations of the sampling grid, during low-flow conditions were similar to those observed in the coastal ocean in Onslow Bay.

Variability of $a_{CDOM}(350)$ in Onslow Bay was much smaller than in the plume (Table 1). Usually, elevated absorption was observed at Masonboro Inlet (the maximum values of $a_{CDOM}(350)$ in Onslow Bay were always recorded at the station OBSB, closest to the shore), and it diminished quickly with distance from shore. CDOM absorption at OB27 varied little and values of $a_{CDOM}(350)$ were minimal or very close to minimum for each respective data series. The low CDOM absorption offshore was similar to absorption levels recorded by Nelson and Guarda, (1995) and Nelson et al., (1998) at the shelf in the Gulf Stream and in the Sargasso Sea. CDOM absorption variability in Onslow Bay roughly followed the cycle observed in the Cape Fear River plume.

Variability of the CDOM spectral slope coefficient in the Cape Fear River plume area was relatively small. For most cruises the values of S were in the range of 0.015–0.018 nm^{-1}. However, small increases of the slope coefficient were observed during low-flow periods in December 2001, June and August 2002. The elevated values of the slope coefficient may be associated with advection of coastal water into the plume area. This water contains

Table 1. Results of descriptive statistical analysis for data collected in the Cape Fear River plume in relation to the river discharge into SAB.

	Cape Fear River Plume												
	$a_{CDOM}(350)$ [m^{-1}]						S [nm^{-1}]						Cape Fear River discharge [m^{3}s^{-1}]
	Min.	Max.	Mean	Median	Std. dev.	n	Min.	Max.	Mean	Median	Std. dev.	n	
Dec. 2001	0.365	1.137	0.742	0.759	0.286	7	0.0178	0.0239	0.0198	0.0188	0.0023	7	32.8
Jan. 2002	1.862	5.830	2.667	2.044	0.429	7	0.0165	0.0170	0.0168	0.0168	0.0002	7	470.2
April 2002	0.573	1.911	1.214	1.195	0.574	7	0.0161	0.0170	0.0165	0.0164	0.0003	7	137.8
June 2002	0.137	0.792	0.428	0.394	0.284	7	0.0163	0.0195	0.0177	0.0173	0.0015	7	27.9
Aug. 2002	0.338	1.133	0.679	0.587	0.334	7	0.0173	0.0186	0.0180	0.0180	0.0006		18.6
Sept. 2002	0.751	1.754	1.306	1.378	0.441	7	0.0169	0.0174	0.0172	0.0172	0.0002	7	74.1
Oct. 2002	0.981	2.706	1.936	2.034	0.669	7	0.0167	0.0169	0.0168	0.0167	0.0001	7	339.8
Nov. 2002	1.244	3.023	2.306	2.621	0.727	7	0.0172	0.0178	0.0175	0.0175	0.0002	7	434.9
All data	0.137	5.830	1.588	1.240	1.203	56	0.0159	0.0239	0.0174	0.0172	0.0013	56	

Table 1 (continued) Results of descriptive statistical analysis in for data collected in the Onslow Bay.

	Onslow Bay											
	$a_{CDOM}(350)$ [m–1]						S [nm^{-1}]					
	Min.	Max.	Mean	Median	Std.dev.	n	Min.	Max.	Mean	Median	Std. dev.	n
Nov. 2001	0.072	0.333	0.130	0.090	0.100	6	0.0174	0.0249	0.0209	0.0203	0.0031	6
Feb. 2002	0.109	0.548	0.255	0.159	0.190	6	0.0128	0.0207	0.0175	0.0181	0.0034	6
April 2002	0.079	0.734	0.305	0.199	0.276	6	0.0178	0.0281	0.0226	0.0215	0.0042	6
June 2002	0.063	0.490	0.160	0.084	0.166	6	0.0151	0.0167	0.0162	0.0163	0.0006	6
Sept. 2002	0.078	0.984	0.349	0.259	0.335	6	0.0176	0.0307	0.0228	0.0215	0.0056	5
Nov. 2002	0.145	0.763	0.286	0.171	0.242	6	0.0157	0.0185	0.0176	0.0180	0.0010	6
Jan. 2003	0.428	0.906	0.736	0.770	0.164	6	0.0165	0.0179	0.0176	0.0179	0.0006	6
All data	0.063	0.984	0.326	0.167	0.285	45	0.0128	0.0307	0.0191	0.0179	0.0037	45

much smaller amounts of CDOM, which may possibly have been photochemically or biologically altered, and is characterized by a steeper absorption spectrum. Changes in the slope coefficient in Onslow Bay did not follow such a clear pattern as in the plume area, although variability was still significant. A distinct feature was the decrease in S values in November 2002 and January 2003, with simultaneous increases in absorption, which suggests a substantial contribution of terrestrial CDOM in Onslow Bay.

Changes in CDOM fluorescence are shown in Figures 5 and 6. These figures show EEM of the two end members in our data set. The fresh water, (salinity = 0) end member is represented by the Black River sample and the oceanic end member is represented by the sample collected in Onslow Bay on September 5 2002, at OB27 ($a_{CDOM}(350)$ = 0.20 m^{-1}, S = 0.0307 nm^{-1}, salinity = 35.98). There were more than two-orders of magnitude difference in fluorescence intensity of the major peak A, which represents terrestrial humic substances. In the fresh water environment this peak is distinct and its shoulders extend into the T peak area.

The C peak, which is attributed to terrestrial fulvic substances, is also clearly distinguished on the Black River spectrum. The most prominent peak visible on the Onslow Bay EMM graph has the emission maximum in the same area as fluorophores characterized for, tryptophan, one of two fluorescent proteins, and labeled as the T peak. We did not performed detailed chemical analysis to characterize the dissolved organic matter in the study area, and therefore we have no evidence of increased relative concentrations of proteins in the clear waters. Although other types

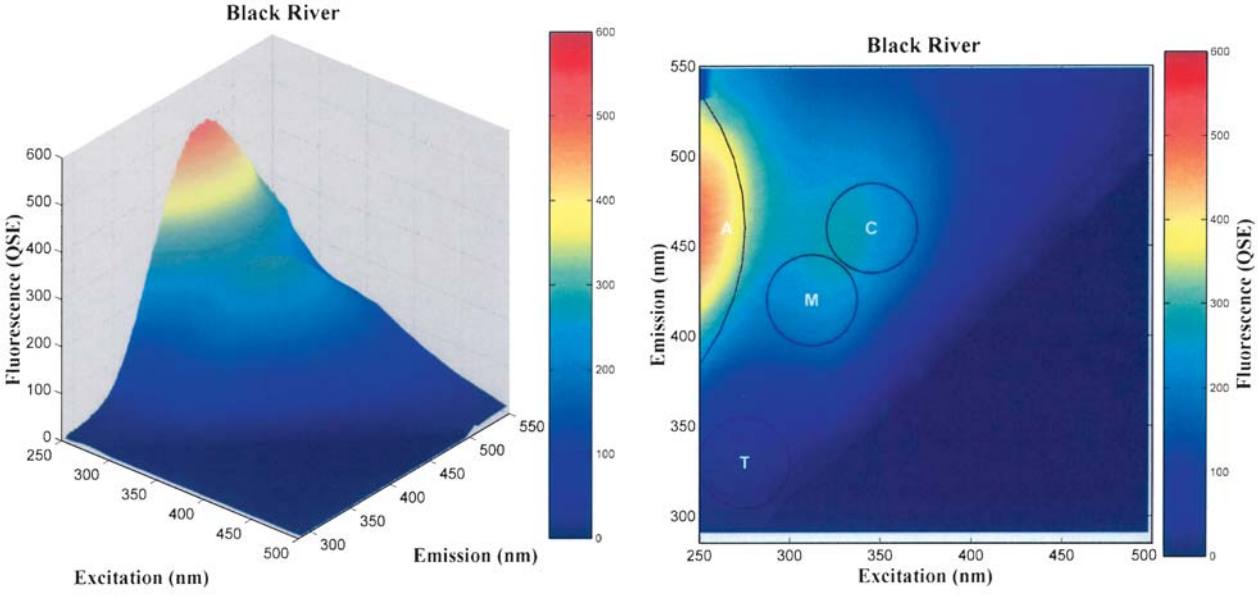

Figure 5. The EEM of the fresh water end member, the sample from Black River, collected in the fall 2001. The A, C, M, and T show locations of the respective fluorescence peaks according to Coble, 1986. The circles centered at peak maxima show the integration cross-section area.

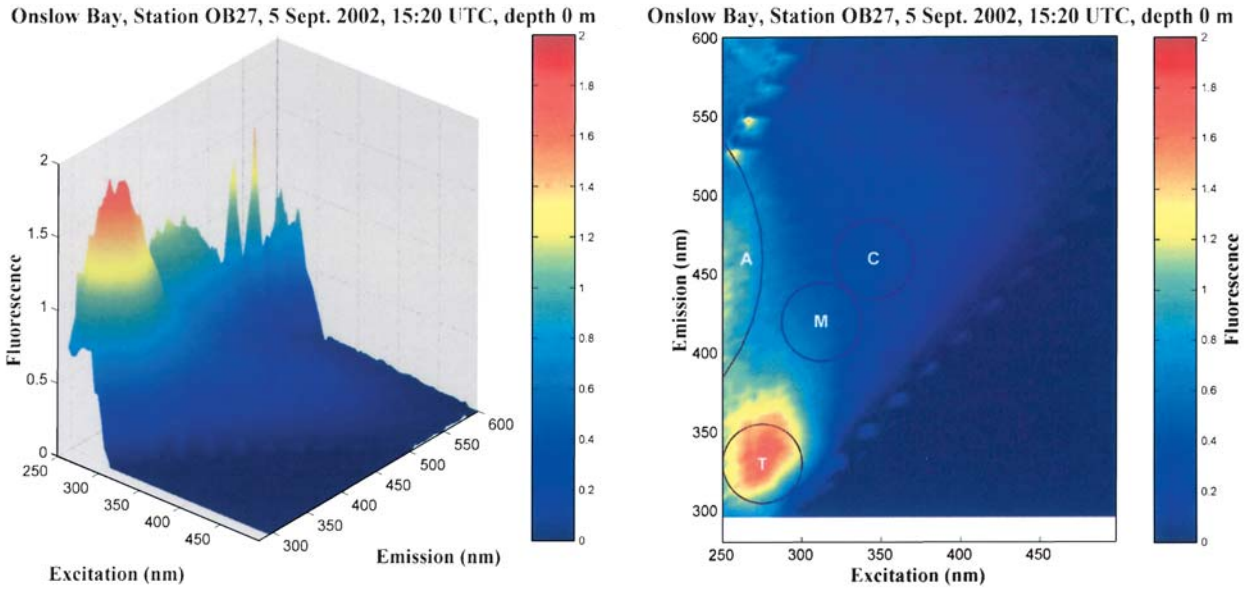

Figure 6. The EEM of the oceanic water end member, the sample of water from Onslow Bay (location, date and time on the graphs), collected in the fall 2001. The A, C, M, and T show locations of the respective fluorescence peaks according to Coble, 1986. The circles centered at peak maxima show the integration cross-section area. The narrow spikes visible on the graph are artifacts due to inefficiency of correction of second order Raman scattering. The low fluorescence signal at ex.275-em.580 nm may be a signal of second order emission by protein-like fluorophores.

of compounds such as phenols exhibit fluorescence in this Ex/Em region, for simplicity we will refer the T peak as the protein-like fluorophores. All other peaks are reduced in their intensities and there are only traces of C and M peaks. Visual inspection of all plotted and ordered EEM spectra from fresh water to ocean end members have shown that with a decrease of absorption/fluorescence intensities, the T peak becomes more prominent. This effect was quantified using the integration option in FLToolbox. Integration areas are shown on the figures as circles or ellipses centered in the respective peak's maxima. The A peak integration area is defined as the part of the ellipse which covers the maximum extent of this peak. In geometrical terms, the integral is the volume of the cylinder cut from the EEM by the respective circle/ellipse, which is its base. The integral of the whole EEM was also calculated. By determining the ratio of the respective integrals of A, C, M and T peaks to that of the whole EMM integral, the percentage contributions of respective peaks to the whole spectrum intensity were calculated. All EEM in our data have been treated the same way. Thus we have a number of parameters, which describe the qualitative changes of CDOM EEM. These parameters were used to calculate relationships between absorption, fluorescence and salinity.

Empirical relationships between absorption, fluorescence and salinity

Regression analysis verified the linear relationship between CDOM absorption and CDOM fluorescence. In a number of previous studies this relationship was usually established between CDOM absorption at the excitation wavelength and fluorescence intensity peak (Ferrari and Tassan, 1991; Hoge et al., 1993; Green and Blough, 1994; Vodacek et al. 1995; Vodacek et al., 1997; Ferrari and Dowell, 1998; Ferrari, 2000; Chen et al., 2002). The high correlation between these two parameters enables the use of fluorescence as a proxy for CDOM absorption. This approach is especially useful in clear waters with low CDOM concentrations, because fluorescence is much more sensitive than absorption measurement, and therefore, it is possible to measure CDOM with improved accuracy. We used the respective peak integrals as a measure of fluorescence intensity and plotted them against the absorption coefficient $a_{CDOM}(350)$, see Figure 7. The regression equation and correlation coefficients are given in Table 2. The logarithm of fluorescence intensities versus absorption coefficients are linearly related with correlation coefficients >0.9. The best fit was obtained between $a_{CDOM}(350)$ and C and M peaks integrals, because the excitation bands for those two peaks are around 350 nm. The A peak was also very well correlated with absorption; however, a larger dispersion of data around the regression curve was observed. The T peak is the least correlated with absorption, because its excitation and emission are located at shorter wavelengths than 350 nm, however, the relationship is still statistically significant.

One of the advantages of the EEM technique is the capability of determining qualitative changes in CDOM composition. Changes in intensities of specific peaks

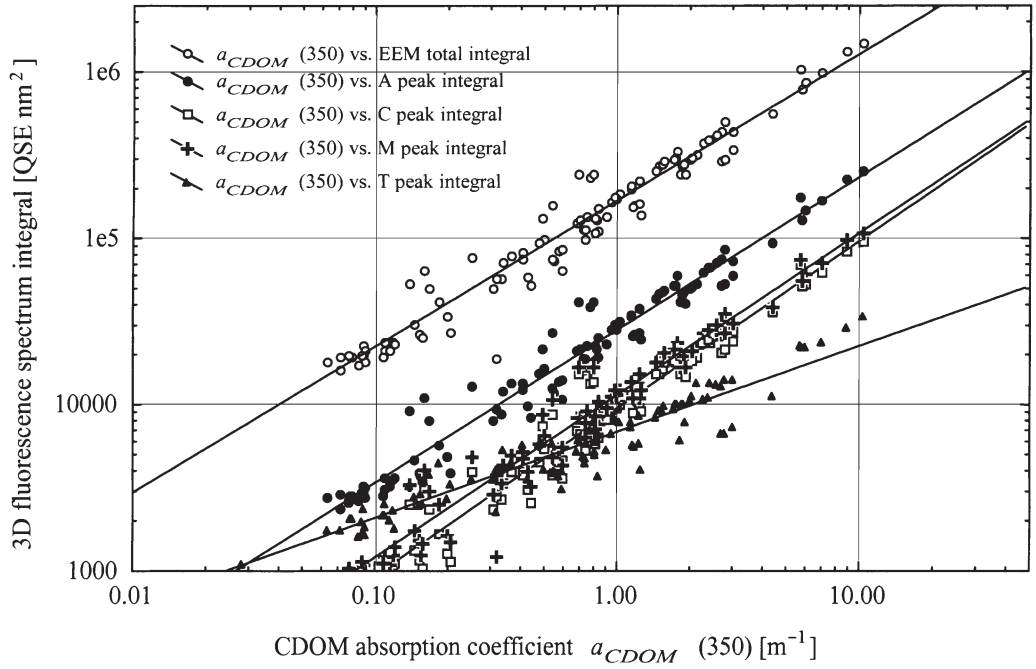

Figure 7. Linear approximation of relationships between respective peaks fluorescence intensities (expressed as the peaks integrals) and CDOM absorption coefficient $a_{CDOM}(350)$.

Table 2. Results of regression analysis between CDOM absorption and respective fluorescence peak intensities.

Variables	Equation	Correlation coefficient	Sample size
$a_{CDOM}(350)$ vs. EEM total intensity	$EEM_{TOT} = 10^{(5.227+0.879(\log_{10}(x)))}$	$r = 0.98$	$n = 105$
$a_{CDOM}(350)$ vs. *A* peak intensity	$A_{peak} = 10^{(4.448+0.92(\log_{10}(x)))}$	$r = 0.98$	$n = 105$
$a_{CDOM}(350)$ vs. *C* peak intensity	$C_{peak} = 10^{(3.976+1.007(\log_{10}(x)))}$	$r = 0.98$	$n = 105$
$a_{CDOM}(350)$ vs. *M* peak intensity	$M_{peak} = 10^{(4.056+0.975(\log_{10}(x)))}$	$r = 0.98$	$n = 105$
$a_{CDOM}(350)$ vs. *T* peak intensity	$T_{peak} = 10^{(3.835+0.517(\log_{10}(x)))}$	$r = 0.95$	$n = 105$

Note: $x = \log_{10}(a_{CDOM}(350))$.

may reflect processes that lead to changes in composition of CDOM. For example, disappearance of the A peak at the fresh and marine water interface at the salinity range 1-5 may provide information relating to the precipitation of the large molecular weight fraction of CDOM, which consists mostly of terrestrial humic acids. Calculated as described above, the percent contribution of the respective peak intensities to the total EEM intensity were related to the CDOM absorption coefficient $a_{CDOM}(350)$, see Figure 8. Three of four analyzed peaks, A, C, and M, show a steady decrease with a decrease of a_{CDOM}. In contrast, the T peak contribution increased significantly with a_{CDOM} decrease. This graph clearly shows the effect of T peak dominance in clear water as observed during qualitative analysis of the EEM. The correlation coefficients and regression equations are given in Table 3. The linear approximation of relationships between the respective peak contribution (in percent) to the total EEM intensity worked reasonably well for the C and M peaks. The regression curves calculated for A and T peaks do not fit the data distribution for high absorption values. This may be an effect of self-absorbing of the emitted energy by CDOM at high concentrations; however, a correction for this effect was applied and with a path length of one cm it is not likely. The high dispersion of data at the low absorption levels visible for the T peak may reflect seasonal variability in the absorption/fluorescence relationship; however, our data set is not adequate to test this hypothesis. Therefore, the linear regression was regarded as a first approximation of the relationship between percent contribution of A and T peak and absorption. We were looking at possible sources of the increased presence of

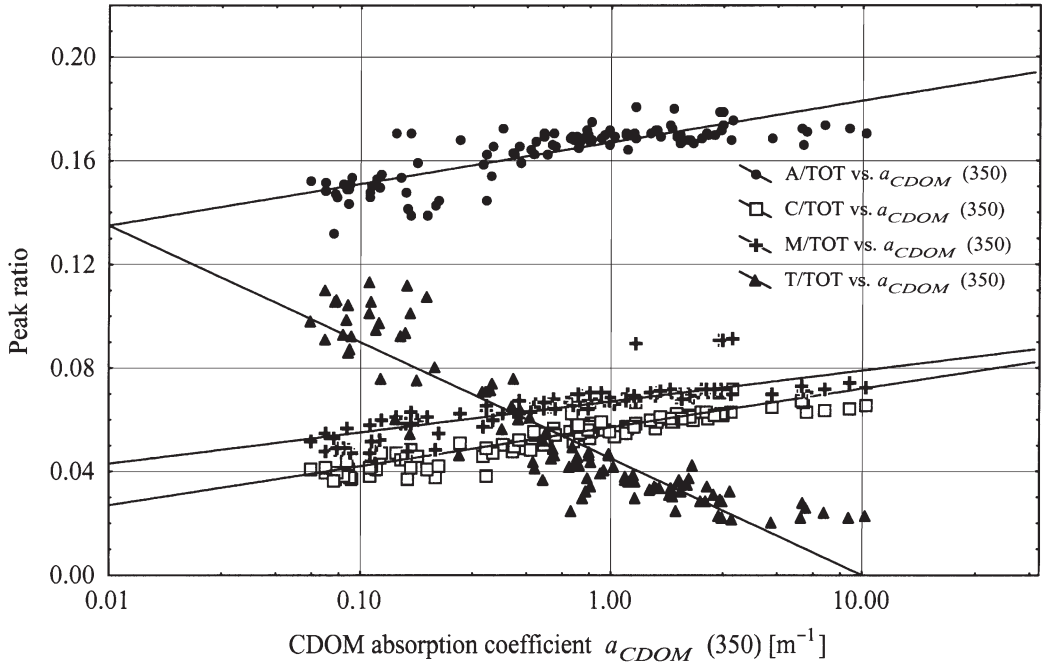

Figure 8. Linear approximation of relationships between ratios of respective peaks intensities to total EEM intensity and CDOM absorption coefficient $a_{CDOM}(350)$.

Table 3. Results of regression analysis between CDOM absorption and percent contribution of respective fluorescence peak intensities to the total EEM intensity.

Variables	Equation	Correlation coefficient	Sample size
$a_{CDOM}(350)$ vs. *A/TOT*	$A/TOT = 0.167 + 0.016(\log_{10}(x))$	$r = 0.79$	$n = 105$
$a_{CDOM}(350)$ vs. *C/TOT*	$C/TOT = 0.057 + 0.015(\log_{10}(x))$	$r = 0.93$	$n = 105$
$a_{CDOM}(350)$ vs. *M/TOT*	$M/TOT = 0.067 + 0.012(\log_{10}(x))$	$r = 0.84$	$n = 105$
$a_{CDOM}(350)$ vs. *T/TOT*	$T/TOT = 0.045 + 0.045(\log_{10}(x))$	$r = -0.89$	$n = 105$

Note: $x = \log_{10}(a_{CDOM}(350))$; *A*, *C*, *M*, *T* – respective fluorescence peak intensity; *TOT* – the total EEM intensity.

the protein-like fluorophores in clear waters; therefore we related the respective peak intensities and respective peak ratios to total EEM intensity. The absolute values of respective peak intensities were linearly related with each other and correlation coefficients were always greater than 0.98 (data not shown). The relationships between each respective peak percent contribution to the total EEM were also very good, but we have shown only the relation of T peak contribution to total EEM intensity compared with the remaining three peak ratios (see Fig. 9). The scatter plot and the fitted linear relationships described above show a trend of increased T peak contribution with a decrease of other peak contributions. However, the T peak contribution is much better correlated with peaks associated with terrestrial humic substances (A and C peak contributions). The correlation of the tryptophan-like fluorophores with marine humic substances (M peak contribution) is much smaller (see Table 4 for details). Also, very high dispersion of data points around the fitted curve of the relationship between *T/TOT* vs. *M/TOT* at the high T peak contribution in clear oceanic waters suggest that tryptophan-like fluorophores are not related with locally produced CDOM.

Mixing is the principal process leading to a decrease of CDOM in the estuary. The overall negative relationship of CDOM absorption and salinity is well known. Figure 10 shows the changes of absorption as a function of salinity. The regression equation is as follows: $a_{DOM}(350) = 26.281 - 0.717$*Salinity; and the correlation coefficient calculated for this relationship was $r^2 = -0.96$, n = 81.

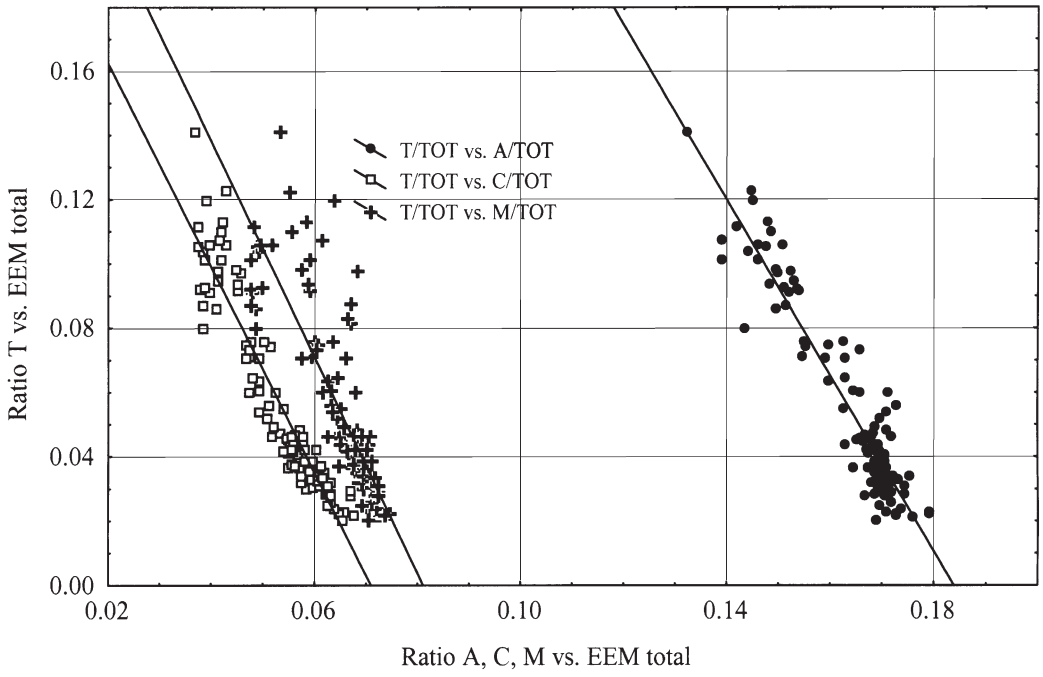

Figure 9. Linear approximation of relationships between ratios of respective CDOM peak intensities to total EEM intensity versus ratio of T peak intensity to total EEM intensity.

Table 4. Results of regression analysis between CDOM absorption and percent contribution respective fluorescence peak intensities to the total EEM intensity.

Variables	Equation	Correlation coefficient	Sample size
T/TOT vs. *A/TOT*	$T/TOT = 0.502 - 2.73x$	$r = -0.93$	$n = 105$
T/TOT vs. *C/TOT*	$T/TOT = 0.226 - 3.183x$	$r = -0.93$	$n = 105$
T/TOT vs. *M/TOT*	$T/TOT = 0.272 - 3.353x$	$r = -0.82$	$n = 105$

Note: $x = A, C, M$, respectively where A, *C*, *M*, *T* – respective fluorescence peak intensity; *TOT* – the total EEM intensity.

A recent study has also shown that DOC is conservatively mixed in the Cape Fear Estuary (Avery et al., 2003). Because CDOM absorption is negatively correlated with salinity, we expected similar results relating the percent contribution of respective peak intensities to the total EEM intensity and salinity, because fluorescence can be regarded as a proxy for CDOM absorption. Figure 11 shows that there is no relationship between salinity and peak ratios along the salinity gradient up to the point where it reaches about 35. When salinity was greater than 35.5, the peak ratios change. The A, M and C peak percent contribution decreases and the T peak contribution significantly increases. This suggests that until CDOM is sufficiently diluted, absorption and fluorescence changes are due to conservative mixing because all of the peaks decrease at approximately the same rate. The effects of other CDOM decomposition processes like photobleaching may be noticeable only when the CDOM is diluted. Other possible explanations of Figure 11 may be linked to the time scales of different decomposition processes. It is estimated that the half-life time of CDOM photobleaching is on the order of several days to several weeks (Vodacek et al., 1997; Del Vecchio and Blough, 2002); mixing in the tidal estuary is much faster. Moreover, the residence time of a given volume of water in the photic zone in a tidal estuary may on the order of minutes due to forcing by tides and wind stress. The UV-photic zone for photobleaching in turbid water rarely exceeds 10 cm, so photobleaching in these waters is inefficient and mixing masks its effect. When water is clear and the photic zone much deeper, photobleaching may be noticeable. The effect of self shading on photobleaching was previously noticed by Del Castillo et al., (1999) and Blough and Del Vecchio (2002).

The slope coefficient is often regarded as a proxy for CDOM composition. Relating the slope coefficient S with absorption coefficient $a_{CDOM}(350)$ and salinity yielded inconclusive results. There is a trend of increased

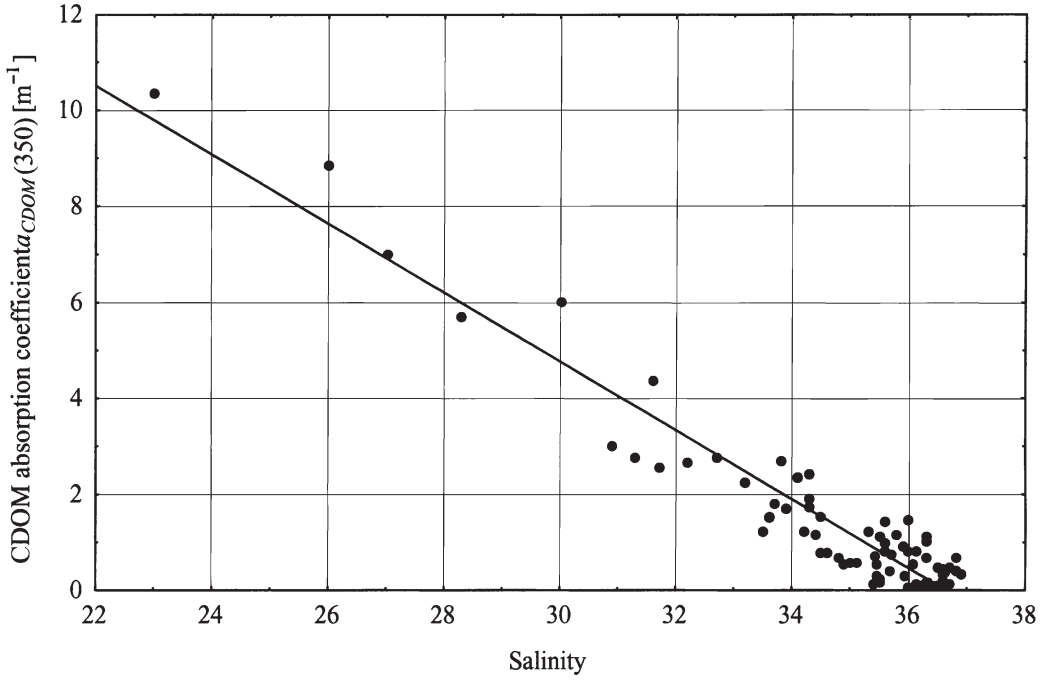

Figure 10. Linear approximation of the relationship between CDOM absorption coefficient and salinity.

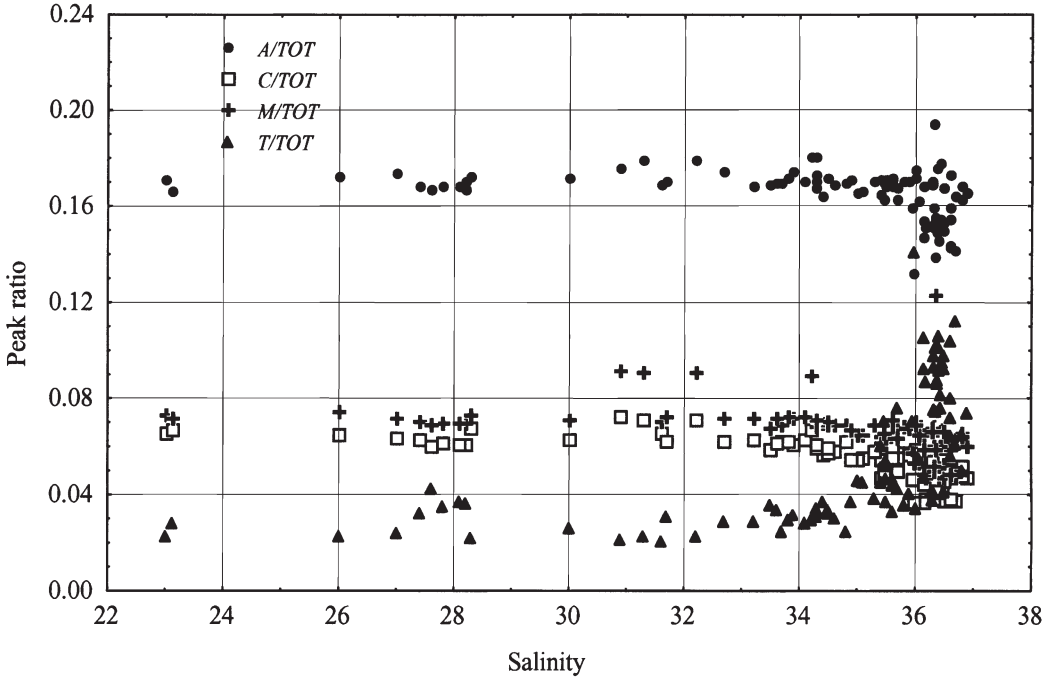

Figure 11. Dispersion plot of ratios of respective peak intensities to total EEM intensity versus salinity.

slope coefficient with a decrease in absorption level; however, the correlation coefficient is much lower than presented above and it is not possible to use a regression equation as the functional relationship. Plotting the slope coefficient against salinity showed that up to approximately the same point, 35.5, there is little change in the slope (see Fig. 12).

Discussion

The Cape Fear River estuary and plume, together with the adjacent coastal ocean, is a unique region to study CDOM dynamics. Within a fairly small area, tens of km, it is possible to measure wide variations in CDOM absorption which cover nearly the whole known variability

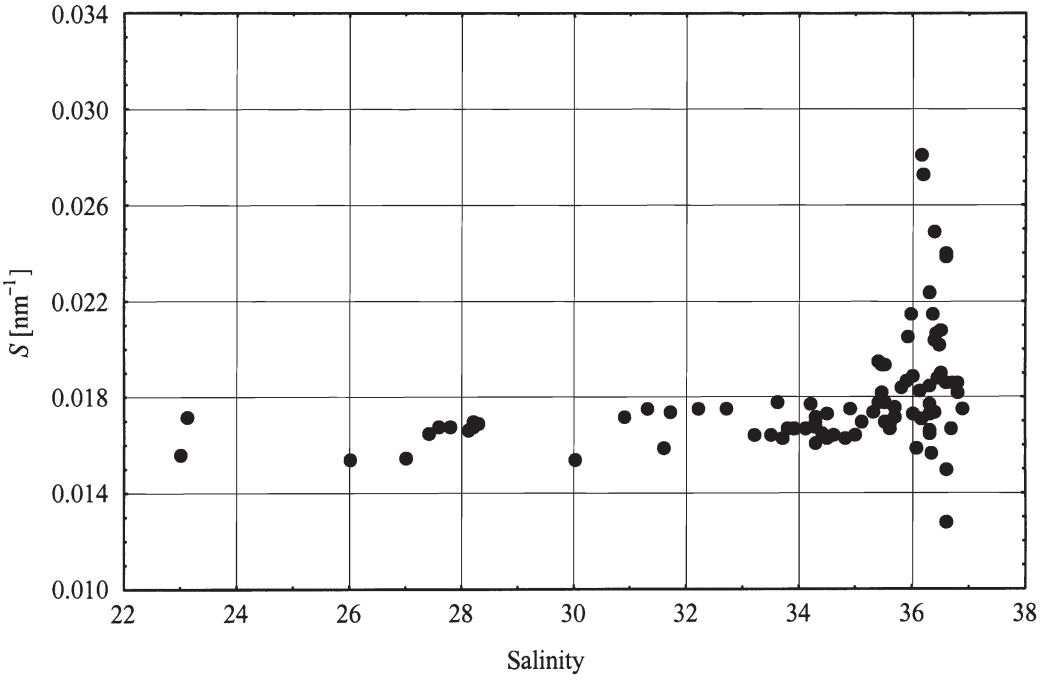

Figure 12. Dispersion plot of the CDOM absorption spectrum slope coefficient *S* versus salinity.

range reported in the literature [see Højerslev (1988) and Blough and Del Vecchio (2002) and references therein]. The most highly absorbing samples found in the Cape Fear estuary are close to the maximum CDOM absorption levels found at the vicinity of river outlets or in marginal seas (see Kowalczuk, 1999; Stedmon et al., 2000). The least-absorbing samples are similar to those reported in the Sargasso Sea and Gulf Stream by Nelson et al., (1998) and Nelson and Guarda (1995). Generally, the CDOM absorption values for the offshore stations in Onslow Bay were lower than those reported for the Mid-Atlantic Bight (DeGrandpre et al., 1996; Vodacek et al., 1997; Boss et al., 2001; Sosik et al., 2001) and were comparable to CDOM absorption levels of the clearest natural waters. The inshore stations of Onslow Bay and the Cape Fear River plume are characterized by high CDOM absorption. CDOM absorption distribution inshore is driven mostly by river flow and mixing with oceanic waters that are influenced by tides and local dynamic processes, in a similar manner to other estuaries on the eastern coast of American continent (Nieke et al., 1998; Johnson et al., 2001; Chang et al., 2002). The calculated Cape Fear River discharge into the SAB during the sampling time span ranges from 470.2 m^3s^{-1} on 29 January 2002, to only 27.9 m^3s^{-1} on 24 June 2002. A preliminary study on Cape Fear River flow and the spatial extent of the riverine plume (Durako et al., 2002) indicated that flow seems to control not only the spatial extent of the riverine plume into the coastal ocean, but also the percent contribution of CDOM, particulate matter and phytoplankton pigment absorption to the total absorption of light in the Cape Fear River area. There is very good agreement between our results and those reported by Nelson and Guarda (1995), but we have observed clear, low-absorption waters much closer inshore than observed further south in the Charleston Gyre area. The low values of CDOM slope coefficient *S*, found in Onslow Bay and in the Cape Fear River plume are very similar to those reported in fresh water environments and estuaries; the high values are very close to those reported for coastal ocean waters in the studies cited above.

The salinity at which the sudden change in CDOM optical properties is observed is called the inflection point (Del Castillo et al., 2000). Blough et al. (1993) and Del Castillo et al. (1999) have reported similar behavior of the spectral slope along the salinity gradient in the Orinoco River plume as we have observed in our data. Similar effects were reported for changes in CDOM emission maximum in Orinoco River plume (Del Castillo et al., 1999) and in West Florida shelf (Del Castillo et al., 2000). The position of the inflection point on the salinity scale depends on the initial concentration of CDOM in the fresh water end-member and should be observed at higher salinities for organic rich rivers. The position of the inflection point observed in our data – 35.5, corresponds very well to observations by Del Castillo et al., (2000) in West Florida Shelf, where outlets of several rivers with high CDOM concentration are located. Our data are also consistent with slope data presented in the study by Nelson and Guarda (1995), where the same pattern in changes in the slope coefficient along the salinity gradient was observed. The sharp change in optical prop-

erties observed in our data and presented in the cited papers may reflect the effect of dilution of terrestrial CDOM into the Gulf Stream, as well as the effect of photobleaching in conditions favorable for longer CDOM exposures to the solar radiation in the mixing zone.

There are few reports that explain changes in EEM shapes. Here, the clearest samples from offshore stations in Onslow Bay were very similar to offshore samples presented in the paper by Coble et al., (1998). Similarly, the shapes of EEM of CDOM collected in more turbid waters were also similar to model EEM for black-water rivers presented by Coble (1996). The systematic decrease of the three principal peaks, A, M, C with decreasing absorption may reflect changes in CDOM concentration with relatively minor changes in composition during transport from the estuarine environment to oceanic waters. However, the relative increase of the T peak, which may be referred to fluorophores similar to the fluorescent proteins, with increased salinity and decreased absorption indicates that this fraction of CDOM may cycle differently than other constituents of the CDOM. Indirect corroboration of our findings comes from the study of Schwarz et al., (2002) conducted in the Baltic Sea. This report presents the application of a Gaussian fitting routine to deconvolute the CDOM absorption spectra into series of Gaussian curves. It was observed that in the Bay of Gdansk, Baltic Sea, that one of those curves, centered around 260 nm, and exhibited a significant positive trend with salinity. Thus, the fraction of CDOM absorbing at that wavelength becomes more prominent. Coincidently, 260 nm is the excitation band of fluorescent proteins. Although the possible pathways of CDOM changes are still little understood, there are several non-mutually exclusive explanations for the patterns in our data: 1) protein-like fluorophores in our samples are a recalcitrant fraction of the CDOM, 2) protein-like fluorophores in our samples are a breakdown product of terrestrial CDOM, 3) protein-like fluorophores are formed in marine environment.

The first possibility may be explained by the fact that under natural conditions there is no light available to directly bleach protein-like fluorophores, which absorbs light below 300 nm. This explanation can be supported by findings by Del Castillo et al., (1999), who reported relative bleaching resistance of fluorophores which absorbs light below 300 nm. Therefore, indirect bleaching processes are involved in their decomposition. Indirect bleaching processes that may involve reactions with reactive-oxygen species or other radicals may be much less efficient than direct bleaching (e.g., Cooper et al., 1989; Blough and Del Vecchio, 2002a; De Mora et al., 2000; Hansell and Carlson, 2002; Holder-Sandvik et al., 2000). Although more specifically designed laboratory experiments are needed to explore the possibility of protein-like fluorophores formation during the decomposition of terrestrial CDOM, the second possibility does not seem likely since we did not observe an increase in absolute values of T but rather a relative increase. Likewise, the same reasoning seems to rule out, or at least limit, the third possibility as well. Therefore, the significant changes observed in our optical data may reflect the dilution of the shelf water mass into the Gulf Stream, where T fluorophores are the dominant moieties. The exact mechanisms by which T becomes dominant are yet to be resolved.

We used the $a_{CDOM}(350)$ to quantify CDOM, because it represents the middle of the UV-A region, where the overlap of the solar irradiance spectrum and a_{CDOM} yields the highest absorption rates and relative photobleaching. We assumed that if a specific fraction of CDOM, represented by different EEM peaks has different photobleaching rates, then it should be reflected in the relationship between CDOM absorption and CDOM fluorescence peak intensities. Results presented in this study showed that our assumption was correct. However, the alternative approach of using absorption integrated over the same range as used for slope calculation instead of $a_{CDOM}(350)$, might improve statistical relationships between integrated absorption and integrated peak intensities especially for those peaks, which are excited at wavelengths different than UV-A. The integrated absorption would probably counter balance the photobleaching effect in the relationship between absorption versus salinity and absorption versus slope. This approach is worth considering in the future studies.

Conclusions

The Cape Fear River estuary and surrounding coastal ocean is a very unique region to study CDOM dynamics. The river and its tributaries are extremely rich in organic matter, and the western-most margins of Gulf Stream can be close to shore, carrying very optically clear waters with low-organic and low-particle contents. Therefore, it is possible to observe exceptionally strong gradients in CDOM absorption and CDOM absorption spectrum slope coefficients within a small geographic area. Using two different analytical techniques we characterized CDOM dynamics in the region and described qualitative and quantitative changes in CDOM composition from its terrestrial source to the oceanic sink. The most important conclusions of this study are as follows:

– Exceptionally high variability of CDOM absorption occurs in the relatively small area of the Cape Fear River estuary and surrounding coastal ocean. The observed range of CDOM absorption coefficients, $a_{CDOM}(350)$, covers nearly the entire known range of CDOM absorption known in the literature: $0.046 = a_{CDOM}(350) = 29.9\ m^{-1}$.

- Variability in the slope coefficient is much lower, especially in the Cape Fear River estuary.
- Local physical processes like: river flow, tides and advection of ocean water into the estuary govern CDOM absorption-coefficient and slope-coefficient dynamics.
- There is a linear relationship between CDOM absorption and CDOM fluorescence intensity.
- Analysis of EEM indicates that three of four principal fluorescence peaks and total integrated fluorescence decrease with decreasing absorption in a similar fashion. In contrast, the protein-like fraction of CDOM (T peak) decreases to a lesser degree than the others.
- Analysis of the percent contribution of fluorescence peak intensities to the total fluorescence along the salinity gradient showed that protein-like fluorophores become the predominant fraction of the CDOM in marine environment.
- The distribution of slope coefficients and the percent contributions of peak- intensities to the total EEM fluorescence both showed that CDOM undergoes conservative mixing until it reaches the ocean. This implies that CDOM is so concentrated in the river and estuary and the time scales of its degradation are such that mixing and other physical processes mask photochemical or biological alteration of its composition until it reaches the seaward edges of the plume.

Acknowledgments

This study was supported by NOAA through the Coastal Ocean Research and Monitoring Program operated by the Center for Marine Science, University of North Carolina at Wilmington. Partial support for this study came from Office of Naval Research through Visiting Scientist Program, Grant No. N00014-02-1-4066. Authors would like to thank Dr. Paula Coble from College of Marine Science, University of South Florida at St. Petersburg and Dr. Robert Chen from University of Massachusetts, Boston for valuable comments on our experimental data. Development of the Fluorescence Toolbox was supported by Office of Naval Research grant N00014-98-1-0530 awarded to Richard Zepp (U.S.E.P.A.) and Mary Ann Moran (University of Georgia).

References

Atkinson, L. P., D. W. Menzel and K. A. Bush, (eds.), 1985. Oceanography of Southeastern U.S. Continental Shelf, Coastal Estuarine Sci. Ser., vol. 2, AGU Washington D.C., 156 pp.

Avery, G. B., J. D. Willey, R. J. Kieber, G. C. Shank and R. F. Whitehead, 2003. The flux and bioavailability of Cape Fear River and rainwater Dissolved Organic Carbon to Long Bay, southeastern United States. Glob. Biogeochem. Cycles **17(2)**, 1042, doi:10.1029/2002GB001964.

Blough N. V., O. C. Zafiriou and J. Bonilla, 1993. Optical absorption spectra of waters from the Orinoco River outflow: Terrestrial input of Coloured Organic Matter to the Caribbean. J. Geophys. Res. **98:** 2271–2278.

Blough N. V., R. Del Vecchio, 2002. Chromophoric DOM in the coastal environment. In: D. Hansell and C Carlson (eds.), Biogeochemistry of marine dissolved organic matter. Academic Press, New York, 509–546.

Boss, E., W. S. Pegau, J. R. Zaneveld and A. H. Barnard, 2001. Spatial and temporal variability of absorption by dissolved material at a continental shelf. J. Geophys. Res. **106(C5):** 9499–9507.

Chen, R. F., Y. Zhang, P. Vlahos and S. M. Rudnick, 2002. The fluorescence of dissolved organic matter in the Mid-Atlantic Bight. Deep Sea Res. II **49:** 4439–4459.

Chang, G. C., T. D. Dickey, O. M. Schofield, A. D. Weidemann, E. Boss, W. S. Pegau, M. A. Moline and S. M. Glenn, 2002. Neashore physical processes and bio-optical properties in the New York Bight, J. of Geophys. Res. **107(C9):** paper 3133.

Coble, P. G., 1996. Characterization of marine and terrestrial DOM in seawater using excitation-emission matrix spectroscopy. Mar. Chem. **51:** 325–346.

Coble, P. G., C. A. Schultz and K. Mopper, 1993. Fluorescence contouring analysis of DOC Intercalibration Experiment samples: a comparison of techniques. Mar. Chem. **41:** 175–178.

Coble, P. G., C. E. Del Castillo and B. Avril, 1998. Distribution and optical properties of CDOM in the Arabian Sea during the 1995 Southwest Monsoon. Deep-Sea Res. II **45:** 2195–2223.

Cooper, W. J., R. G. Zika, R. G. Petasne and A. M. Fischer, 1989. Sunlight Induced Photochemistry of Humic Substances in Natural Waters: Major reactive species. In: P. MacCarthy and I. H. Suffett, (eds.), Influence of aquatic humic substances on fate and treatment of pollutants, American Chemical Society, Advances in Chemistry **219:** 333–362.

DeGrandpre, M. D., A. Vodacek, R. K. Nelson, E. J. Bruce and N. V. Blough, 1996. Seasonal seawater optical properties of the U.S. Middle Atlantic Bight. J. Geophys. Res. **101:** 22,727–22,736.

Del Castillo, C. E., P. G. Coble, J. M. Morell, J. M. Lopez. and J. E. Corredor, 1999. Analysis of the optical properties of the Orinoco River plume by absorption and fluorescence spectroscopy. Mar. Chem. **66:** 35–51.

Del Castillo, C. E., F. Gilbes, P. G. Coble and F. E. Müller-Karger, 2000. On the dispersal of riverine colored dissolved organic matter over the West Florida Shelf. Limnol. Oceanogr. **45(6):** 1425–1432.

Del Vecchio R. and N. V. Blough, 2002a. Photobleaching of chromophoric dissolved organic matter in natural waters: kinetics and modeling. Mar. Chem. **78:** 231–235.

Del Vecchio, R. and N. V. Blough, 2002b. Influence of ultraviolet (UV) radiation on the Chromophoric Dissolved Organic Matter (CDOM) in natural waters. In: F. Ghetti and J. F. Bornman, (eds.), Environmental UV Radiation: Measurement and Assessment. Impact on Ecosystem and Human Health, NATO ASI SERIES, 2001, *Accepted to publication*.

De Mora, S., S. Demers and M. Vernet (eds.), 2000. The effects of UV radiation in the marine environment. Cambridge University Press, Cambridge UK, 334 pp.

Durako M. J., P. Kowalczuk, J. J. Souza, M. A. Mallin, M. R. McIver, 2002. Spatial and temporal variation in CDOM in a coastal blackwater river plume. In: Steven G. Ackleson; (ed.), Proceedings of Ocean Optics XVI Conference, paper no. 18, 10 pp., Santa Fe, New Mexico, USA, 18–22 November 2002.

Duursma, E. K., 1965. The dissolved organic constituents of seawater. In: J. P. Riley and G. Skirrow (eds.) Chemical Oceanography, 1, Academic Press, London, pp. 433–475.

Ferrari, G., 2000. The relationship between chromophoric dissolved organic matter and dissolved organic carbon in the European Atlantic coastal area and in the West Mediterranean Sea (Gulf of Lions). Mar. Chem. **70(4):** 339–357.

Ferrari, G. and S. Tassan, 1991. On the accuracy of determining light absorption by "yellow substance" through measurements of induced fluorescence. Limnol. Oceanogr. **36(4):** 777–786.

Ferrari, G. and M. Dowell, 1998. CDOM absorption characteristics with relation to fluorescence and salinity in coastal areas of the southern Baltic Sea. Est. Coast. Shelf Sci. **47(1):** 91–105.

Garver, S. A. and D. A. Siegel, 1997. Inherent optical property inversion of ocean color spectra and its biogeochemical interpretation. 1. Time series from Sargasso Sea. J. Geophys. Res. **102:** 18607–18625.

Green, S. A. and N. V. Blough, 1994. Optical absorption and fluorescence properties of chromophoric dissolved organic matter in natural waters. Limnol. Oceanogr. **39:** 1903–1916.

Grzybowski, W., 2000. Effect of short-term irradiation on the absorbance spectra of the chromophoric organic matter dissolved in the coastal and riverine waters. Chemosphere, **40:** 1313–1318.

Hansell, D. A. and C. A. Carlson (eds.), 2002. Biogeochemistry of marine dissolved organic matter. Academic Press, New York, 774 pp.

Harvey, G. B., D. A. Boran, L. A. Chesal and J. M. Tokar, 1983. The structure of marine fulvic and humic acids. Mar. Chem. **12:** 119–132.

Hoge, F. E., R. N. Swift, J. K. Yungel and A. Vodacek, 1993. Fluorescence of dissolved organic matter: A comparison of North Pacific and North Atlantic Oceans during April 1993. J. Geophys. Res. **98(C12):** 22779–22787.

Holder-Sandvik, S. L., P. Bilski, J. D. Pakuski, C. F. Chigell and R. B. Coffin, 2000. Photogeneration of singlet oxygen and free radicals in dissolved organic matter isolated from the Mississippi and Atchafalaya river plumes. Mar. Chem. **69:** 139–152.

Højerslev, N. K., 1988. Natural occurrences and optical effects of Gelbstoff. Rep. 50, Inst. of Phys. Oceanogr., Univ. of Copenhagen, Copenhagen, 30 pp.

Højerslev, N. K., 1989. Surface water-quality studies in the interior marine environment of Denmark. Limnol. Oceanogr. **34(8):** 1630–1639.

Jerlov, N. G., 1976, Marine Optics. Elsevier, New York, 231 pp.

Johnson, D. R., A. Weidemann and R. Arnone, 2001. Chesapeake Bay outflow plume and coastal upwelling events: Physical and optical properties. J. Geophys. Res. **106 (C6):** 11613–11622.

Kahru, M. and B. G. Mitchell, 1999. Empirical chlorophyll algorithm and preliminary SeaWiFS validation for the California Current. Int. J. Remote Sens. **20(17):** 3421–3429.

Kahru, M. and B. G. Mitchell, 2001. Seasonal and non-seasonal variability of satellite-derived chlorophyll and colored dissolved organic matter concentration in the California Current. J. Geophys. Res. **106(C2):** 2517–2529.

Kieber, D. J., B. M. Peake and N. M. Scully, 2003. Reactive oxygen species in aquatic ecosystems. In: E. W. Helbling and H. Zagarese (eds.), UV effects in aquatic Organisms, Royal Society of Chemistry, Cambridge, UK, 251–288.

Kieber, R. J., L. H. Hydro and P. M. Seaton, 1997. Photooxidation of triglycerides and fatty acids in seawater: Implication toward the formation of marine humic substances. Limnol. Oceanogr. **42(6):** 1454–1462.

Kirk, J. T. O., 1994. Light and Photosynthesis in Aquatic Ecosystems, 2nd ed. Cambridge University Press., New York, 509 pp.

Kowalczuk, P., 1999. Seasonal variability of yellow substance absorption in the surface layer of the Baltic Sea. J. Geophys. Res. **104(C12):** 30 047–30 058.

Kowalczuk, P., M. Darecki, J. Olszewski and S. Kaczmarek, 2003. Empirical relationships between Coloured Dissolved Organic Matter (*CDOM*) absorption and apparent optical properties in Baltic Sea waters. International Journal of Remote Sensing (in press).

Mallin, M. A., J. M. Burkholder, L. B. Cahoon and M. H. Posey, 2000. North and South Carolina Coast, Mar. Poll. Bull. **41(1–6):** 56–75.

Mopper, K. and D. J. Kieber, 2002. Photochemistry and the cycling of carbon, sulfur, nitrogen and phosphorus, In: D. A. Hansell and C.A. Carlson, (eds.), Biogeochemistry of Marine Dissolved Organic Matter, Academic Press, New York, 455–507.

Moran, A. M., W. M. Sheldon and R. G. Zepp, 2000. Carbon loss and optical changes during long-term photochemical and biological degradation of estuarine dissolved organic matter. Limnol. Oceanogr. **45(6):** 1254–1264.

Morel, A. and L. Prieur, 1977. Analysis in variation of ocean color. Limnol. Oceanogr. **22(4)**: 709–722.

Nelson, J. R. and S. Guarda, 1995. Particulate and dissolved spectral absorption on the continental shelf of the southeastern United States. J. Geophys. Res. **100(C5):** 8715–8732.

Nelson, N. B., D. A. Siegel and A. F. Michaels, 1998. Seasonal dynamics of colored dissolved organic matter in the Sargasso Sea. Deep Sea Res. **45:** 931–957.

Nieke, B., R. Reuter, R. Heuermann, H. Wang, M. Babin and J. C. Therriault, 1998. Light absorption and fluorescence of chromophoric dissolved organic matter (CDOM) in the St. Lawrence Estuary (Case 2 waters). Cont. Shelf Res. **17(3):** 235–252.

Pempkowiak, J., 1988. The Distribution, Origin and Properties of Humic Acids in the Baltic Sea. Ossolineum, Wroc3aw, Poland, 146 pp, (in Polish).

Rochelle-Newall, E. J., T. R. Fisher, C. Fan and P. M. Glibert, 1999. Dynamics of chromophoric dissolved organic matter and dissolved organic carbon in experimental mesocosm. Int. J. Remote Sens. **20(3):** 627–641.

Rochelle-Newall, E. J. and T. R., Fisher, 2002a. Production of chromophoric dissolved organic matter fluorescence in marine and estuarine environments: an investigation into a role of phytoplankton. Mar. Chem. **77:** 7–21.

Rochelle-Newall, E. J. and T. R., Fisher, 2002b. Chromophoric dissolved oragnic matter and dissolved organic carbon in Chesapeake Bay. Mar. Chem. **77:** 23–41.

Shao, C., W. J. Cooper, and D. R. S. Lean, 1994. Singlet oxygen formation in lake waters from mid-latitudes. In: Helz, G. R., R. G. Zepp, D. G. Crosby (eds.), Aquatic and Surface Photochemistry, Lewis Publishers, Ann Arbor, MI, 215–221.

Sosik, H. M., R. E. Green, W. S. Pegau and C. S. Roesler, 2001.Temporal and vertical variability in optical properties of New England shelf waters during late summer and spring. J. Geophys. Res. **106(C5):** 9455–9472.

Stedmon, C. A., S. Markager and H. Kaas, 2000. Optical properties and signatures of Chromophoric Organic Dissolved Matter (CDOM) in Danish Coastal waters. Est. Coast. Shelf Sci. **51:** 267–278.

Stedmon, C. A. and S. Markager, 2001. The optics of chromophoric dissolved organic matter (CDOM) in the Greenland Sea: An algorithm for differentiation between marine and terrestrially derived organic matter. Limnol. Oceanol. **46(8):** 2087–2093.

Schwarz, J. N, P. Kowalczuk, S. Kaczmarek, G. F. Cota, B. G. Mitchell, M. Kahru, F. P. Chavez, A. Cunningham, D. McKee, P. Gege, M. Kishino, D. A. Phiney, R. Raine, 2002. Two models for absorption by coloured dissolved organic matter (CDOM). Oceanologia **44(2):** 209–241.

Tranvik, L. J., 1993. Microbial transformation of liable dissolved organic matter into humic-like matter in seawater. FEMS Microbiol. Ecol. **12:** 177–183.

Tranvik, L. J. and S. Bertilsson, 2001. Contrasting effects of solar UV radiation on dissolved organic sources for bacterial growth. Ecol. Lett. **4:** 458–463.

Twardowski, M. S. and P. L. Donaghay, 2001. Separating in situ and terrigenous sources of absorption by dissolved organic materials in coastal waters. J. Geophys. Res. **106(C2):** 2545–2560.

Twardowski, M. S. and P. L. Donaghay, 2002. Photobleaching of aquatic dissolved materials: Absorption removal, spectral alteration, and their interrelationship. J. Geophys. Res. **107(C8):** art. no. 3091.

Vodacek, A., F. E. Hoge, R. N. Swift, J. K. Yungel, E. T. Peltzer and N. V. Blough, 1995. The use of in situ and airborne fluorescence measurements to determine UV absorption coefficients and DOC concentrations in surface waters. Limnol. Oceanogr. **40:** 411–415.

Vodacek, A., N. V. Blough, M. D. DeGrandpre, E. T. Peltzer and R. K. Nelson, 1997: Seasonal variation of CDOM and DOC in the Middle Atlantic Bight: Terrestrial inputs and photooxidation. Limnol. Oceanogr. **42(2):** 674–686.

Whitehead, R. F. and S. de Mora, 2000. Marine Photochemistry and UV radiation. In: Hester, R. E. and R. M. Harrison (eds.), Issues in Environmental Science and Technology No. 14, Causes and Environmental Implications of Increased UV-B Radiation, Royal Society of Chemistry, 37–60.

Whitehead, R. F., S. de Mora, S. Demers, M. Gosselin, P. Monfort and B. Mostajir, 2000. Interactions of ultraviolet-B radiation, mixing, and biological activity on photobleaching of natural chromophoric dissolved organic matter: A mesocosm study. Limnol. Oceanogr. **45(2):** 278–291.

Willey, J. D. and L. P., Atkinson, 1982. Natural fluorescence as a tracer for distinguishing between piedmont and coastal plain river water in the near shore waters of Georgia and N. Carolina. Est. Coast. Shelf Sci. **14:** 49–59.